Design and Performance of a Packaged InP Wavelength Meter

R. G. Broeke,[1] D. Melati,[2] F. Morichetti[2]

[1] Bright Photonics BV, Netherlands, ronald.broeke@brightphotonics.eu, www.brightphotonics.eu

[2] Politecnico di Milano, Dipartimento di Elettronica, Informazione e Bioingegneria, via Ponzio 34/5, 20133 Milano, Italy

Over the past years many users of multi-project wafer (MPW) runs successfully demonstrated their Photonic ICs in the lab. However, for this generic technology to be successful outside a university environment it is pivotal to fully package PICs. This paper demonstrates a fully-packaged wavelength-meter prototype fabricated in an InP MPW run, as well as a design tolerance analysis. The device measures wavelength shifts across a 3 nm band with the potential to go below femtometer accuracy, centered anywhere in the 1465 to 1600 nm wavelength range. Additionally, we report on a novel integrated on-chip temperature sensor.

Introduction

Photonics has been identified by the European Union and industry alike as a key-enabling technology of the future, i.e. it is one of the drivers for innovation, high-tech start-ups, high added value and job creation in small and medium sized companies. One of the most interesting developments over the last few years is the rise of the generic foundry model for Photonic Integrated Circuits (PICs) in Europe [1]. The model provides cost sharing for PIC users at fabrication level, process level and wafer level and it established a software design environment with Photonic Design Kits (PDK). It reduces the financial and technological threshold for access to PIC prototypes by several orders of magnitude. This model is the vehicle by which PICs find their way to a multitude of diverse new applications. One of the first fields that benefits of this development is Sensing. This paper presents a wavelength sensor fabricated on an InP multi-project wafer (MPW) run [2], fiber pigtailed and fully packaged. It is the first report of a device from the InP MPW runs that demonstrates the full chain from photonic building blocks (BB) to a characterized prototype, including a tolerance analysis at circuit level.

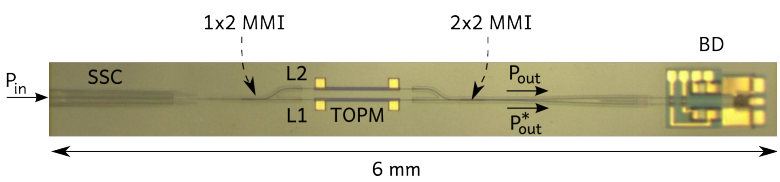

Figure 1: Photograph of the fabricated 6 mm long device.

Figure 2: The packaged device.

Device description

The wavelength meter is based on the well established interferometric effect: An optical component splits a light beam in two. Each beam travels along a path of optical length $n_{\text{eff}} \cdot L_1$ and $n_{\text{eff}} \cdot L_2$, respectively, where L_1 and L_2 are the geometrical path lengths and n_{eff} the effective refractive index of the paths. After traversing the paths a second component interferometrically recombines the beams. The phase relation at recombination depends on the optical path length difference $\Delta L = L_2 - L_1$ as $\Delta\theta = n_{\text{eff}} \cdot \Delta L/\lambda$. The output field, in complex numbers and omitting the time dependence of the electromagnetical wave, becomes $E_{\text{out}} = E_{\text{in}} \exp(i\Delta\theta)$. Here E_{in} denotes the amplitude of the input field, λ the wavelength and we omit loss. For $\Delta L \neq 0$ the output field amplitude E_{out}, and its intensity $P_{\text{out}} = [\text{Re}(E_{\text{out}})]^2$, become a nearly sinusoidal function of λ with a period or Free Spectral Range (FSR) of $\lambda_{\text{FSR}} = \lambda^2/(n_g \Delta L)$, where $n_g = n_{\text{eff}} - \lambda \cdot \frac{\delta n_{\text{eff}}}{\delta \lambda}$ represents the group index.

The wavelength meter exploits precisely this wavelength dependency of P_{out}. However, a fluctuation of input power $P_{\text{in}} = |E_{\text{in}}|^2$ also modulates P_{out}, hence balanced detection (BD) is used to distinct between power fluctuations in the input and a wavelength shift. BD combines P_{out} and its inverted companion $P^*_{\text{out}} = [\text{Im}(E_{\text{out}})]^2$, also generated at interference, into balanced parameter $B = (P_{\text{out}} - P^*_{\text{out}})/(P_{\text{out}} + P^*_{\text{out}})$ independent of P_{in}.

The wavelength meter has been realized (Fig. 1) as a PIC on the FhG-HHI InP foundry in the form of a 1x2 Mach-Zehnder Interferometer (MZI) consisting of a 1x2 multi-mode interference (MMI) coupler in combination with a 2x2 MMI. The signals in the two outputs of the 2x2 MMI are inverted with respect to each other, i.e. two sinus-like functions 180 degrees out of phase, and fed into the balanced detector (BD) on the right side. The optical input on the left has an integrated spot-size converter (SSC) matching the circular 10 um mode diameter of standard fiber. The arm-lengths in the MZI were optimized for a FSR = 10 nm at $\lambda = 1550$ nm. Both MZI arms contain a Thermo-Optical Phase Modulator (TOPM), which can tune the position of the MZI transfer function across a full λ_{FSR} period. The MMIs, BD, SSC, TOPMs and interconnecting waveguides were available as foundry-compatible GDS building blocks in the mask-layout design environment. Figure 2 shows the package of the anti-reflection coated device.

Tolerance analysis

The MZI performance is sensitive to random variations of the optical and geometrical design parameters, for example as caused by fabrication. A tolerance analysis with an optical circuit simulator in the design flow is able to perform a statistical analysis of the MZI. Figure 3(a) shows the wavelength meter's circuit model in Aspic$^{\text{TM}}$[3], assembled with BBs from the FhG-HHI library. The library describes each BB by a realistic model containing information of its statistical behavior. Figure 3(b) shows the effects of tolerances on the MZI transmission through a number of random device realizations; It considered the variability of loss and splitting ratio's of the 1x2 MMI (α_{12}, K_{12}) and of the 2x2 MMI (α_{22}, K_{22}), together with a variability of waveguide loss (α_{wg}) and n_{eff}. The circuit simulator processes these data through numerical approaches or analytical models [4]. This provides information on several statistical quantities such as the expected value and the variance of the circuit response, and a yield estimation and sensitivity analysis.

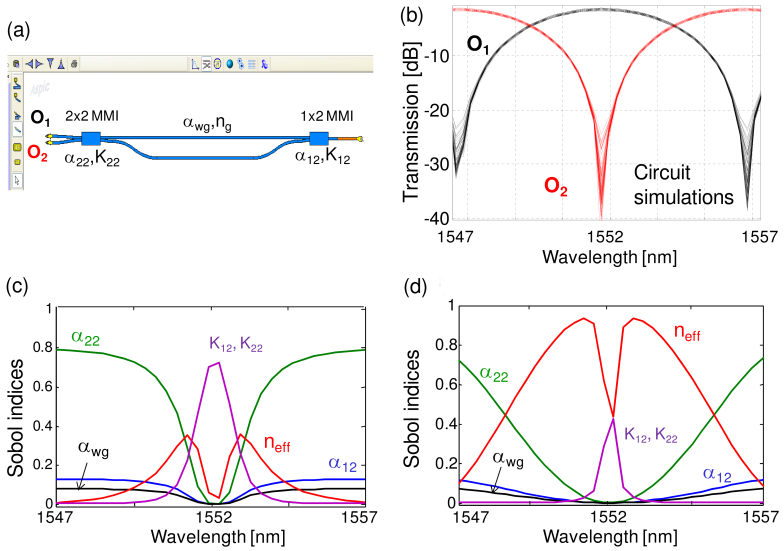

Figure 3: (a) Schematic of the MZI wavelength meter designed in Aspic™; (b) Effects of tolerances of the BB optical parameters on the MZI transmission at output ports O_1 (black curves) and O_2 (red curves). (c) and (d) show the sensitivity analysis (Sobol indices) of the MZI considering a thermal stabilization of 0.1 °C (c) and 0.5 °C (d).

A sensitivity analysis for finding the most critical parameters of the circuit can be done effectively by Sobol indices [5], which express the contribution of each parameter to the total variance of the process: The higher the Sobol index (between 0 and 1) is for a parameter, the more critical the parameter is to device performance. For instance, Fig. 3(c) shows that MZI extinction at port O_2 at λ = 1552 nm is strongly sensitive to the MMI splitting ratios (K_{12} and K_{22}, purple curves); conversely, at the MZI transmission maxima (1547 nm and 1557 nm), excess loss (α_{22}, green curve) of the 2x2 MMI becomes dominant. These results assumed thermal stabilization within ±0.1 °C, corresponding to a n_{eff} fluctuation of about ±2e-5. For a coarser thermal stability (e.g. ±0.5 °C, ±1e-4 n_{eff} fluctuations) n_{eff} is the most critical parameter at most wavelengths, as shown in Fig. 3(d).

Measurement results

For characterization of the packaged device a tunable laser served as the optical source. An optical attenuator followed by a polarization controller fixed the optical input power to the package. Two Keithly source meters simultaneously read the currents from the balanced photo-diodes while the laser scanned the wavelength of the input light. A TEC controller stabilized the temperature of the device at 20 °C. Figure 4 presents the periodic diode response versus λ for TE and TM polarization, normalized at maximum current. The response is displayed in dB scale to better show the symmetrical response of the device, though this is not critical in this sensing application. The extinction ratio is around 25 dB, but due to the resolution of the data this is not always clear from the plot. The efficiency from fiber power to diode current was measured at $R_{\text{fd}} = 0.29$ A/W for λ = 1520 to 1575 nm. For λ down to 1465 nm this was still 0.21 A/W. We expect the device to operate well above 1600 nm based on other data, resulting in a large 150 nm operational span. The FSR = 10 nm at λ = 1550 nm, as designed. TE and TM curves are

displaced with respect to each other, because the waveguides are not polarization independent. Figure 3 shows the excellent balanced detection response B. Wavelength sensing operates in the bandwidth of about $\lambda_{bw} = 3\,\text{nm}$ on any steep section of the curves, as indicated by the dotted rectangle on the TM curve. The sensitivity of the wavelength meter follows from $\lambda_s = \lambda_{bw} \cdot \text{NEP} \cdot f/(R_{fd} \cdot P_{in})$, where NEP is the noise equivalent power of the diodes and f the sampling rate frequency. At $f = 10\,\text{kHz}$, $P_{in} = -10\,\text{dBm}$, and $\text{NEP} \approx 0.2\,\text{pW}/\sqrt{\text{Hz}}$ we find $\lambda_s \approx 2\,\text{fm}$. With higher input power and/or lower f a sensitivity of attometers seems within reach.

The above sensitivity is an ideal case without temperature fluctuations, among others. However, the MZI has a novel feature: an integrated temperature sensor. Its sensitivity is $10\,\text{mV}/^\circ\text{C}$ and multiple of these sensors can be integrated on a single chip. Therefore, accurate real time calibration for local temperature changes in the MZI is feasible.

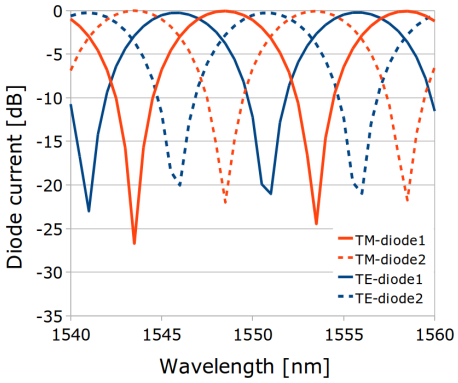

Figure 4: Measured balanced-detector photocurrents across two MZI periods.

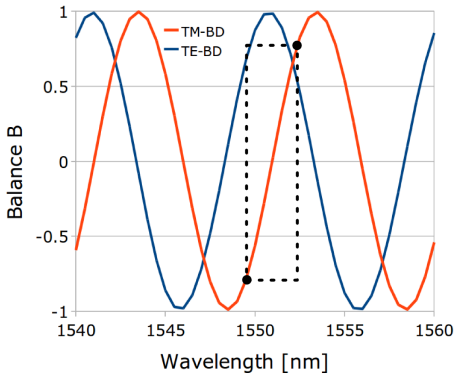

Figure 5: Measured balance B in the wavelength meter.

Acknowledgements

The authors wish to thank Warsaw University of Technology and Krzysztof Anders for characterization support, Andrea Melloni and Davide Cassano from Politechnico de Milano, and Arjen Bakker and Remco Stoffer from PhoeniX Software for software support, FhG-HHI for their excellent foundry services, Detlef Pech for packaging, and Francisco Soares for the valuable discussions. The research leading to these results has received funding from EU FP7/2007-2013 under grant agreement ICT 257210 PARADIGM.

References

[1] M. Smit, X. Leijtens, E. Bente, J. van der Tol, H. Ambrosius, D. Robbins, M. Wale, N. Grote, and M. Schell. Generic foundry model for InP-based photonics. *IET Optoelectronics*, 5(5):187–194, 2011.

[2] Francisco M. Soares, Klemens Janiak, Jochen Kreissl, Martin Moehrle, and Norbert Grote. Semi-insulating substrate based generic inp photonic integration platform. In *Proc. SPIE 8767, Integrated Photonics: Materials, Devices, and Applications II*, page 10.1117/12.2017431, May. 22 2013.

[3] Aspic^{TM} Filarete srl, Italy, www.aspicdesign.com; Phoenix BV, Netherlands, www.phoenixbv.com.

[4] F. Morichetti D. Cassano and A. Melloni. Statistical analysis of photonic integrated circuits via polynomial-chaos expansion. In *Proceed. of Advanced Photonics*, page JT3A.8. Optical Society of America, Jul. 17–Jul. 19 2013.

[5] I.M. Sobol. Global sensitivity indices for nonlinear mathematical models and their monte carlo estimates. *Mathematics and Computers in Simulation*, 55(1–3), 2001.